

Temperature dependence of the bond-stretching phonon anomaly in $\text{YBa}_2\text{Cu}_3\text{O}_{6.95}$

D. Reznik,^{1,2} L. Pintschovius,¹ J. M. Tranquada,³ M. Arai,⁴ Y. Endoh,⁵ T. Masui,⁶ and S. Tajima⁶

¹Forschungszentrum Karlsruhe, Institut für Festkörperphysik, D-76121 Karlsruhe, Germany

²Laboratoire Léon Brillouin, CE Saclay, F-91191 Gif-sur-Yvette, France

³Condensed Matter Physics and Materials Science Department, Brookhaven National Laboratory, Upton, New York 11973, USA

⁴Materials and Life Science Division, J-PARC Center, Japan Atomic Energy Agency, Tokai-mura, Naka-gun, Ibaraki-ken 319-1195, Japan

⁵Synchrotron Radiation Research Center, Japan Atomic Energy Agency, Hyogo 679-5148, Japan

⁶Department of Physics, Osaka University, Toyonaka, Osaka 560-0043, Japan

(Received 4 July 2008; published 11 September 2008)

We report the results of a detailed inelastic neutron-scattering study of renormalization of the bond-stretching phonons in optimally doped $\text{YBa}_2\text{Cu}_3\text{O}_{6+x}$ (YBCO). In agreement with previous work, this renormalization is strongest halfway to the zone boundary in the [010] direction where it manifests itself as a transfer of phonon spectral weight from ~ 60 to ~ 50 meV. Phonon renormalization begins on cooling from well above the superconducting transition temperature, T_c , but strongly accelerates at T_c . In contrast with the $\text{La}_{2-x}\text{Sr}_x\text{CuO}_4$ system, where a similar longitudinal phonon anomaly occurs, the anomaly in YBCO appears to extend in the transverse direction along the branch that connects the longitudinal mode at the in-plane wave vector $\mathbf{q}_{\text{in}}=(0,0.25)$ and the transverse bond-stretching mode at $\mathbf{q}_{\text{in}}=(0.25,0.25)$. Therefore, phonon renormalization in $\text{YBa}_2\text{Cu}_3\text{O}_{6.95}$ seems to be consistent with a quasi-one-dimensional behavior.

DOI: 10.1103/PhysRevB.78.094507

PACS number(s): 74.25.Kc, 63.20.kd, 74.72.Bk

I. INTRODUCTION

It is well known that conventional superconductivity is mediated by phonons. In fact, conventional superconductors with the highest T_c 's tend to exhibit exceptionally strong electron-phonon coupling. Phonon renormalization at specific wave vectors (Kohn anomalies) appears in the phonon dispersions of many of these compounds in agreement with calculations based on the local-density approximation (LDA). In the case of the cuprates, LDA calculations¹⁻³ predict neither any significant Kohn anomalies nor phonon-mediated high T_c superconductivity. For this reason, the most intense research effort has focused on purely electronic mechanisms. However, some researchers have interpreted recent photoemission experiments in terms of renormalization of electronic excitations by phonons.⁴⁻⁶ Also, inelastic neutron and x-ray scattering experiments on the high T_c cuprates found huge softening and broadening of the bond-stretching phonons.⁷⁻¹¹

In the most thoroughly studied family, $\text{La}_{2-x}\text{Sr}_x\text{CuO}_4$ (LSCO), strong phonon renormalization has been observed⁷⁻⁹ in the vicinity of the reduced in-plane wave vector $\mathbf{q}_{\text{in}}=(0.25,0)$ [in units of $(2\pi/a, 2\pi/a)$ where a is the near-neighbor Cu-Cu distance]. The effect is strongest at low temperatures and in compositions that exhibit the so-called stripe order,¹²⁻¹⁴ where the wave vector at which it occurs is compatible with the charge order.⁷ In contrast, this effect disappears at the nonsuperconducting extremes of doping. Detailed \mathbf{q} -dependent studies revealed that the underlying electronic instability is two dimensions in nature; i.e., for $\mathbf{q}_{\text{in}}=(0.25,K)$, it is peaked at $K=0$ with a full width at half maximum of ~ 0.15 r.l.u.¹⁵

In previous work on $\text{YBa}_2\text{Cu}_3\text{O}_{6.95}$, Chung *et al.*¹⁶ identified an anomaly in the anisotropic bond-stretching modes, with a strong temperature dependence below T_c . Subsequent work by Pintschovius and co-workers,^{17,18} involving a com-

bination of measurements and model calculations, resolved the character of the anomaly. In particular, it was shown that the softening of the bond-stretching mode at the zone boundary would cause it to cross the lower-lying bond-bending mode; however, because the modes have the same symmetry, they mix and repel one another rather than actually crossing. Nevertheless, the hybridization of the modes causes the atomic displacement character associated with the bond-stretching mode to shift to the lower branch as the wave vector varies from zone center to zone boundary. For this reason the phonon anomaly appears as a temperature-dependent transfer of spectral weight between branches at the wave vector halfway to the zone boundary for vibration along the b axis (parallel to the Cu-O chains); there is no significant temperature dependence at zone center or zone boundary.

In the present paper, we report a careful study of the temperature dependence of the phonon anomaly around $\mathbf{q}_{\text{in}}=(0,0.25)$ in $\text{YBa}_2\text{Cu}_3\text{O}_{6.95}$. We confirm the observation of Chung *et al.*¹⁶ that there is a strong softening for $T < T_c$; however, we show that there is also a gradual change at temperatures up to several times T_c . We also investigated the behavior of the anomaly in the transverse direction along $\mathbf{q}_{\text{in}}=(H,0.25)$. The softened mode appears to remain over a substantial range of H . We discuss the implications of this observation for the dimensionality of the electronic instability.

II. EXPERIMENTAL DETAILS

Inelastic neutron-scattering measurements were performed on a composite sample of optimally doped $\text{YBa}_2\text{Cu}_3\text{O}_{6.95}$ ($T_c=93$ K); details of the sample are given elsewhere.¹⁹ The neutron experiments were carried out on the 1 T triple-axis spectrometer at the ORPHEE reactor of the Laboratoire Leon Brillouin at Saclay, France. The (220)

reflection of a Cu crystal was used as the monochromator. Pyrolytic graphite (PG) (002) was used for the analyzer crystal. Both were horizontally and vertically focusing. A PG filter in the final beam suppressed higher order contaminations. We note that the detwinned sample used in a previous study^{17,18} was no longer available because this sample disintegrated on warming following the initial experiment.

III. EXPERIMENTAL RESULTS

A. Oxygen phonon branches and their determination

The experiments focused on the Cu-O in-plane bond-stretching vibrations in the $[100]$ and $[010]$ directions because it was known from previous investigations^{16–18} that these branches show an anomalous dispersion at low temperatures. These earlier studies had shown that the energies of the bond-stretching modes lie in the range of 55–75 meV for $T > 200$ K but extend to below 50 meV at low temperatures. Therefore, we investigated an energy range from 42 to 80 meV. There are in total 13 phonon branches in this energy range. All these modes have predominantly oxygen character because oxygen has a much lighter mass than all the other atoms in $\text{YBa}_2\text{Cu}_3\text{O}_{6+x}$ (YBCO). Four of these branches are associated with in-plane Cu–O bond-stretching vibrations. In the in-plane high-symmetry directions, $[1\ 0\ 0]$ and $[0\ 1\ 0]$, two modes have longitudinal and two have transverse character. The two branches of longitudinal character differ by the relative phase of the atomic displacements in the nearest-neighbor CuO_2 planes (bilayer): the in-phase vibrations have Δ_1 symmetry and the out-of-phase vibrations have Δ_4 symmetry, as illustrated in Fig. 1. Their frequencies are very similar because the coupling of the oxygen displacements within the bilayer is quite weak.

The anomaly is observed in both the Δ_1 and Δ_4 bond-stretching modes; however, the bulk of the measurements in the present study was done on phonons with Δ_4 symmetry. The reason is as follows: phonons of Cu–O bond-stretching character will hybridize with other modes of the same symmetry when they are close in energy. This hybridization causes phonon branches that might otherwise cross to avoid crossing, but in doing so it mixes the character of the modes. Within the energy range we study, the Δ_1 planar modes can mix with a chain mode, while the chain mode does not couple to Δ_4 and is weak in intensity where Δ_4 is strong.

To reiterate, the hybridization leads to a so-called anticrossing of phonon branches. This means that two phonon branches belonging to the same group-theoretical representation are not allowed to cross each other but will be separated by a finite-energy anticrossing gap at all wave vectors. If the two branches have different dispersions, there will nevertheless be a crossing in the following sense: there will be a gradual exchange of eigenvectors around the q value where the two branches would have crossed in the absence of any hybridization. This phenomenon is of particular importance for the understanding of the bond-stretching phonon dispersion at low temperatures (see below).

Assignments of phonon peaks were based on shell-model calculations, which reproduce peak positions and intensities in several Brillouin zones with good, although not perfect,

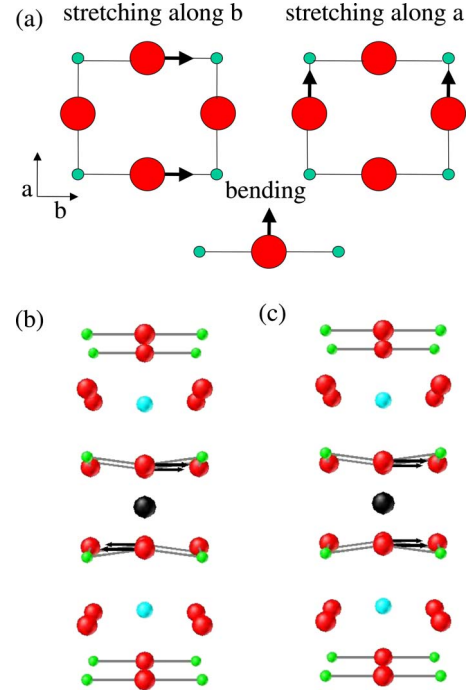


FIG. 1. (Color online) (a) Schematic of the bond-stretching (and bending) vibrations along a and b directions. Small green/Large red circles represent Cu/O, respectively. Eigenvectors of the zone center (b) Δ_4 and (c) Δ_1 bond-stretching phonons.

accuracy.^{17,18} Based on these calculations, measurements were made around the $(3,0,0)$ (Δ_1 symmetry) or the $(3,0,2)$ reciprocal-lattice point (Δ_4 symmetry). The twinning of our present sample complicated the assignment of the neutron peaks to the a^* or the b^* direction. Figure 2 shows how the stretching phonon dispersions previously measured on a detwinned sample along the $[100]$ and $[010]$ directions are superimposed when the twinned sample is measured. Due to the different lattice constants,²⁰ measurements of the scattering intensity at nominal momentum transfers $I(H,0,L)$ actually probe a superposition of intensities at two different wave vectors, $I(0.99H,0,L) + I(0,1.01H,L)$, as illustrated in Fig. 2. Thus, the choices of measuring at $\mathbf{Q} = (3,0,L) - \mathbf{q}$ or $\mathbf{Q} = (3,0,L) + \mathbf{q}$ each have different advantages and disadvan-

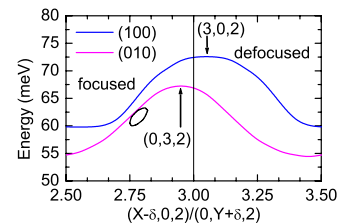


FIG. 2. (Color online) Dispersion relation of the out-of-phase Cu–O bond-stretching vibrations in optimally doped YBCO as seen on a twinned sample. The energies are plotted against the nominal wave vector calculated from an average lattice constant $a_{\text{ave}} = (a + b)/2$. The actual wave vectors for the scattering from each of the two twin domains differ by $2\delta = 2\pi/a - 2\pi/b$. The arrows show the zone center for phonons propagating along the a^* or the b^* direction. The ellipsoid depicts the instrumental resolution.

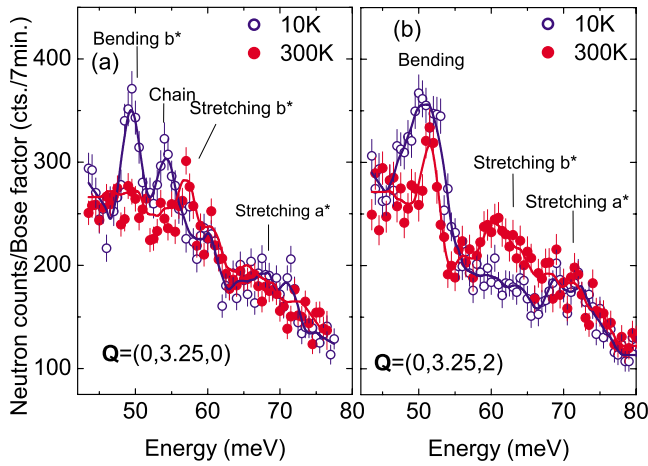


FIG. 3. (Color online) Comparison of phonon spectra measured at $\mathbf{q}=(0,0.25,0)$ in the defocused condition and $T=10$ and 300 K for (a) Δ_1 and (b) Δ_4 . Intensities have been divided by the Bose factor.

tages. For the former choice, focusing leads to relatively narrow phonon lines, but the peaks for the two orthogonal modes are close in energy for q values around 0.25; whereas for the latter choice the resolution function is tilted opposite to the dispersion (defocused condition), but the energy separation of the modes is larger. Both configurations have been tried to elucidate the behavior of the bond-stretching phonons. To simplify the notation going forward, we will only refer to the b^* contribution to the scattering intensity because that is where strong phonon renormalization appears.

B. Temperature-dependent studies

Figure 3 shows the data taken at the wave vector $\mathbf{q}=(0,0.25,0)$ at 300 and 10 K for the Δ_1 symmetry in (a) and Δ_4 in (b). Here we are in the defocused condition of Fig. 2, which provides a better energy separation between the bond-stretching modes along a^* and b^* . In the Δ_4 symmetry of (b), there is a pronounced shift of spectral weight from 60 to 50 meV when the temperature is lowered. In the Δ_1 symmetry of (a), the shift of spectral weight is more complicated because of the anticrossings mentioned above. Still, the data show that some weight is transferred from ~ 57 meV to two phonon peaks at 53 and 49 meV. These effects appear only in the bond-stretching phonons along b^* . No similar effects are observed for the bond-stretching mode along a^* , which remains at ~ 70 meV as the temperature changes.

At the wave vectors $\mathbf{Q}=(0,3,L)-\mathbf{q}$, focusing leads to a better energy resolution. Representative scans are shown in Fig. 4. At $\mathbf{Q}=(0,2.75,2)$, the contributions from the a^* and b^* directions show up at nearly the same energy at $T=200$ K. The pronounced intensity loss on cooling seen in Fig. 4(b) corresponds very well to that observed at $\mathbf{Q}=(0,3,25,2)$ in Fig. 3(b). In addition, one can see that there is no apparent peak broadening or softening at any temperature, indicating that all of the lost intensity must be shifted out of the measured energy window. This intensity loss rap-

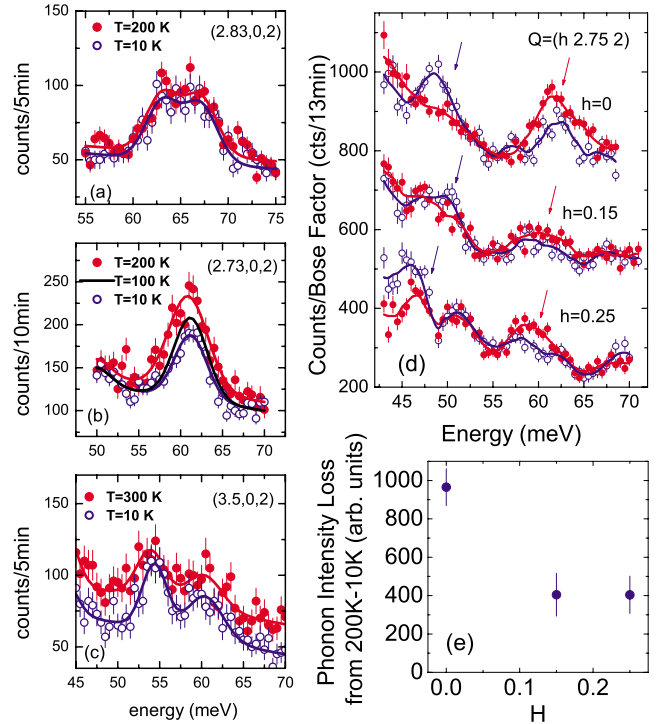


FIG. 4. (Color online) Energy scans taken at different temperatures. [(a)–(c)] Lines correspond to fits with 1 or 2 G. The 100 K data points have been omitted for clarity from (b). The double peak in (a) and (c) corresponds to the a^* mode (the higher energy peak) and the b^* mode (the lower energy peak). These two peaks merge to a single one in (b). (d) Data were taken with the final energy $E_f=13.4$ meV for $\hbar\omega \geq 46$ meV and with $E_f=12.5$ meV $43 \leq \hbar\omega \leq 48$ meV. The 12.5 meV data were corrected for the different resolution volume by multiplying by $(13.4/12.5)^2$. The resulting intensities were averaged in the overlapping energy range (46.5–48 meV). The 200 K data were divided by the Bose factor and 23 counts were subtracted to correct for the temperature dependence of the background. Blue/red arrows (on the right/left side) indicate intensity gain/loss. (e) Integrated intensity loss from 200 to 10 K integrated around the 60 meV peak in the data shown in (d).

idly disappears when going toward the zone center, as illustrated in Fig. 3(a), where the spectra at $\mathbf{Q}=(0,2.83,2)$ are nearly temperature independent except for a small change in the background. The temperature effect also diminishes rapidly toward the zone boundary at $\mathbf{q}=(0,0.5,0)$, as shown in Fig. 4(c), where the dominant temperature effect is a shift in the background. The width in \mathbf{q} of the temperature effect was found to be ~ 0.15 r.l.u (FWHM).

We also followed the temperature dependence in greater detail at a limited number of points. One set of measurements was done for the Δ_1 symmetry at $\mathbf{Q}=(0,3,25,0)$, corresponding to Fig. 3(a), for the energies 49, 53, and 57 meV. The data points in Fig. 5(a) represent the difference between the intensity at 57 meV and the average of intensities at 53 and 49 meV. Taking the difference was necessary to remove the temperature dependence of the background. In the Δ_4 symmetry, we measured only the intensity at $\mathbf{Q}=(0,2.75,-2)$ at 60 meV plus the temperature dependence of the background. The intensity at 60 meV minus the background is plotted in Fig. 5(b). It is clear that although the temperature

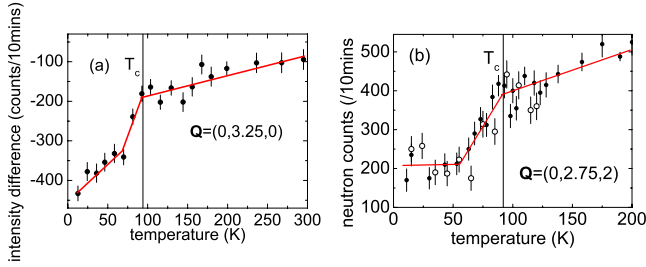


FIG. 5. (Color online) Temperature dependence of phonon-scattering intensity. (a) Difference between the intensity at 57 meV and the average of intensities at 53 and 49 meV at $\mathbf{Q}=(0, 3.25, 0)$. (b) Background-subtracted intensity at $\mathbf{Q}=(0, 2.75, 2)$ at 60 meV. Open and solid circles represent different datasets (see text).

evolution begins well above T_c , the most pronounced change occurs below T_c .

C. Dependence on transverse q

In addition to the high-symmetry [010] direction, we also investigated the evolution of the phonon anomaly at wave vectors $\mathbf{Q}=(H, 2.75, 2)$ for $H > 0$. Based on the previous studies and calculations, we know that in the direction of increasing H the longitudinal modes propagating along [010], L[010], connect to the transverse [110] modes, T[110]. Along the zone boundary, this connection was shown explicitly in measurements by Reichardt (see Fig. 2 of Ref. 20). Similarly, he showed that T[010] modes [which have zero structure factor for $\mathbf{Q}=(0, 2+K, 2)$] connect to L[110]. Here, although we measured in a region only halfway to the zone boundary rather than at the zone boundary, we expect lattice dynamics to be qualitatively similar. It is important to remember that, in a twinned crystal such as ours, we also pick up contributions from another Brillouin zone at $\mathbf{Q}=(2.75, K, 2)$. Starting from $K=0$, the L[100] again connects to T[110] and T[100] connects to L[110]. Shell-model calculations predict a smaller structure factor of the L[100]–T[110] branch in this Brillouin zone than of the L[010]–T[110] branch along $\mathbf{Q}=(H, 2.75, 2)$. Thus, we believe that most of the stretching phonon intensity away from the [100] direction comes from $\mathbf{Q}=(H, 2.75, 2)$, but this prediction still needs to be verified on a large detwinned sample.

Figure 4(d) shows the behavior at $\mathbf{Q}=(H, 2.75, -2)$ for $0 \leq H \leq 0.25$, i.e., along the line in reciprocal space such that \mathbf{q} moves from the [010] to the [110] direction. The spectral weight redistribution from ~ 60 to ~ 48 meV remains significant all the way to $H=0.25$. As a measure of this, Fig. 4(e) shows the loss of weight from the 60 meV feature as a function of H .

It is not straightforward to quantify the \mathbf{q} dependence of the underlying electronic instability in the transverse direction based on the variation in the phonon effect because electron-phonon coupling is expected to change as a function of \mathbf{q} with the changing phonon eigenvector. Furthermore, our peak assignments are complicated by the difficulty in separating the branches connecting to L[010] and L[100] due to twinning. Nevertheless, if we make the assumption that the electron-phonon coupling strength of the bond-stretching

mode is proportional to the volume change around the Cu ion due to the oxygen displacements of the phonon eigenvector, our shell-model simulation shows that electron-phonon coupling should be reduced by approximately a factor of 2 from $\mathbf{q}_{\text{in}}=(0, 0.25)$ to $\mathbf{q}_{\text{in}}=(0.25, 0.25)$. This is roughly what we see in Fig. 4(e), suggesting that the electron-phonon coupling does not depend strongly on the transverse \mathbf{q} component.

An alternative way to quantify the phonon anomaly is to look at the frequency shift of the transferred spectral weight. It is clear from Fig. 4(d) that this frequency shift (from the red to blue arrows) is not strongly dependent on H . Hence, we again conclude that the electronic instability underlying the phonon renormalization does not depend strongly on H .

IV. DISCUSSION AND CONCLUSIONS

How can we understand the phonon spectral weight redistribution that we have observed? If we consider only the change along the high-symmetry [010] direction in jumping from high temperature to low, the interpretation appears straightforward. A softening of the bond-stretching mode, by as much as 14 meV, occurs over a narrow range of \mathbf{q} (in the longitudinal direction). This softening would cause the bond-stretching mode to touch or cross the lower-energy bond-bending mode; however, because of hybridization of the two modes, a transfer of spectral weight (and vibrational character) between the modes is observed rather than a crossing.

In order to explore the extent to which the observed phenomena can be simulated by conventional lattice dynamics, we performed shell-model calculations with a program that allows the force constants to be adjusted in a way that selectively affects the frequency of modes with Cu–O in-plane bond-stretching character only. The simulations gave the following results: a softening of the bond-stretching mode leads to an exchange of eigenvectors with lower phonon branches and thereby to a redistribution of intensities, as we have proposed; however, in addition to the weight transfer, the simulations also yield a significant shift in energy of the bond-stretching mode. The latter point is inconsistent with the experimental observations, such as Fig. 4(b), where we see loss of intensity with cooling for the bond-stretching mode, but no real change in the mode energy. Thus, the simulated scenario does not adequately describe the experiment.

A variation on this model would be to assume that softening occurs inhomogeneously, so that some weight stays at the original mode energy and, for some reason, we do not resolve the weight corresponding to the softened component. We note that Stercel *et al.*²¹ have made a similar proposal of mixed inhomogeneous character to describe the behavior of the bond-stretching branch in underdoped $\text{YBa}_2\text{Cu}_3\text{O}_{6+x}$; however, another important effect in the underdoped regime is a large difference between the dispersions of the modes polarized along a^* and b^* , as reported²² for $\text{YBa}_2\text{Cu}_3\text{O}_{6.6}$.

Likewise, the relatively weak change in the spectral weight loss at ~ 60 meV as a function of transverse \mathbf{q} , as illustrated in Fig. 4(e), seems difficult, if not impossible, to explain within the framework of conventional lattice dynamics. With the anomalous temperature evolution as an impor-

tant caveat, the phonon anomaly in the [010] direction at low T resembles very much the Kohn anomalies observed in one-dimensional (1D) conductors above the charge-density-wave (CDW) transition.²³ This would mean that the phonon anomaly is a precursor phenomenon to a charge-inhomogeneous state. One might conjecture that the effect is related to flat parts of the Fermi surface (FS) of oxygen chain character.²⁴ Density functional theory calculations¹ indeed predict a local frequency minimum at $\mathbf{q}=(0,0.25,0)$ in a Δ_1 branch with primarily bond-stretching chain O character. This feature is not unexpected in view of the one-dimensional nature of the Cu-O chains and may be related to static charge modulations detected within the Cu-O chains by scanning tunneling microscopy (Refs. 25 and 26); however, we emphasize that the phonon anomaly is best observed in a branch of Δ_4 symmetry for which the chain O displacements are zero. This fact excludes a trivial relationship with chain O related electronic states.

Recent angle-resolved photoemission measurements²⁷⁻²⁹ have demonstrated that the bonding FS is nested with the wave vectors $\mathbf{q}=(0,0.25,L)$ along b^* and $(0.2,0,L)$ along a^* . Thus Fermi-surface nesting could be consistent with the observed phonon effect along b^* , but it is not obvious why it should not also be present along a^* . LDA calculations³ also predict a nearly nested FS for the bilayer bonding band with the nesting wave vectors near $\mathbf{q}=(0,0.3,L)$ and $(0.25,0,L)$, whereas the antibonding FS is not nested. LDA-based phonon-dispersion or linewidth calculations, which include first-principles calculation of electron-phonon coupling strength, are in a good agreement with our 200 K phonon data but fail to reproduce the observed phonon renormalization at lower temperatures.¹ Apparently, the LDA significantly underestimates electron-phonon coupling strength for the stretching (and also for the bond-buckling) phonon.

There are two different ways in which one can try to relate the effects to the stripe picture. In the first, one assumes that the strong electron-phonon coupling is associated with screening the formation of the charge stripes, with the phonon anomaly occurring at the wave vector corresponding to the stripe modulation.^{30,31} In that case, the phonon anomaly along b^* would imply stripes running along the a axis. If the length of the stripes exceeds a few unit cells, oxygen vibrations must be in phase in the direction perpendicular to the propagation vector in order to match the quasi-two-dimensional correlations. Since this condition is violated if the transverse component of the phonon wave vector is not equal to zero, the phonon anomaly should rapidly disappear in the transverse \mathbf{q} direction. This is observed in LSCO (Ref. 15) but not in YBCO. As shown in Fig. 4(e), the intensity loss at ~ 60 meV decreases rather slowly in the transverse direction. Moreover, the volume change around the Cu ion due to the oxygen displacements of the phonon eigenvector decreases also when going away from the [010] direction, thereby reducing the electron-phonon coupling strength, which at least partly explains the reduction in the effect. Another problem with connecting the anomaly to the stripe modulation wave vector is that it requires the charge modulation to occur in a direction orthogonal to the magnetic modulation indicated by magnetic scattering studies.³²⁻³⁵

An alternative scenario within the stripe picture is a CDW instability along charge stripes.³⁶ In this case, the formation

of metallic stripes would make the electronic properties of a cuprate similar to that of one-dimensional conductors. Based on the anisotropy of the dynamic magnetic susceptibility in YBCO,³²⁻³⁵ one would expect these 1D systems to run parallel to the Cu-O chains and along the b axis. It follows³⁷ that the Fermi surface associated with these 1D systems would form sheets split about the antinodal point $\mathbf{k}=(0.5,0,0)$, so that nesting of these sheets would be relevant to the strength of the electron-phonon coupling. As noted above, the \mathbf{q} for the phonon anomaly seems to be consistent with $2k_F$ in the b^* direction from photoemission work.²⁷⁻²⁹ It appears from the photoemission results that the nesting condition in YBCO remains valid even when a substantial transverse component is added to \mathbf{q} , and this might explain the observed weak sensitivity to transverse \mathbf{q} . A more careful analysis would require consideration of nesting effects involving electronic states with energies differing by 50–60 meV, comparable to the phonon energy. Nesting conditions at E_F would only be directly relevant if the energy of the phonon mode was approaching zero.

We should note that this same picture, involving phonons coupling to low-energy electronic excitations *within* charge stripes, can also be applied to LSCO and $\text{La}_{2-x}\text{Ba}_x\text{CuO}_4$ (LBCO). In the case of LBCO with $x=1/8$, it appears that the \mathbf{q} for the phonon anomaly⁷ corresponds to $4k_F$ based on photoemission results.³⁸ Of course, it is then unclear why the phonon anomaly is more sensitive to transverse \mathbf{q} in LBCO than in YBCO.

Returning to YBCO, Chung *et al.*¹⁶ reported that the phonon intensity shift in Δ_1 symmetry occurs only below T_c , which appears to contradict our result that the phonon effect begins well above T_c . The contradiction disappears if one considers a difference in energy range between the two studies. In generating Fig. 5(a), we included the peak at 49 meV, which is below the lower cutoff of 51 meV for analysis of Chung *et al.*¹⁶ It turns out that if we neglect the intensity of the 49 meV peak, the temperature change occurs only below T_c .

The strong influence of T_c (Fig. 5) on the phonon renormalization shows that it is intimately connected with superconductivity. Of course, the dynamic magnetic susceptibility also changes dramatically at T_c for optimally doped YBCO,³⁹⁻⁴¹ so the connection with superconductivity is not unique. The phonon effect is not simply a result of the superconductivity, as it is already detectable well above T_c and well above the pseudogap opening temperature (which is very close to T_c at optimal doping in YBCO). We propose here the possibility that the phonon interacts with an electronic collective mode that develops above T_c , but whose damping by the Stoner continuum is reduced as a consequence of superconductivity. It would be particularly interesting to explore whether a collective mode with the correct dispersion and coupling to superconductivity can exist in the fluctuating stripe picture. A new study of charge excitations at finite momentum by Wakimoto *et al.*⁴² provides intriguing evidence in this direction.

Comparing optimally doped YBCO (O6.95) to underdoped O6.6,²² we find that the low T phonon dispersion of O6.6 shows an anomaly similar to that observed in O6.95, although not quite as clearly. Reinspection of temperature-

dependent data also revealed a significant temperature effect, which was overlooked in Ref. 22 because it does not show up as a peak shift but, again, as a shift of spectral weight. This indicates that the phonon anomaly reported in this paper is not restricted to optimally doped compositions.

In summary, we observed a pronounced temperature-dependent effect in the Cu-O in-plane bond-stretching vibrations. Although the underlying mechanism is not fully clear yet (though we have discussed several scenarios), the experi-

mental results are clear evidence for a strong electron-phonon coupling, especially because there is a fingerprint of T_c in the temperature evolution of the phonon anomaly.

ACKNOWLEDGMENTS

J.M.T. is supported at Brookhaven by the Office of Science, U.S. Department of Energy under Contract No. DE-AC02-98CH10886.

-
- ¹K.-P. Bohnen, R. Heid, and M. Krauss, *Europhys. Lett.* **64**, 104 (2003).
- ²F. Giustino, M. L. Cohen, and S. G. Louie, *Nature (London)* **452**, 975 (2008).
- ³R. Heid, K.-P. Bohnen, R. Zeyher, and D. Manske, *Phys. Rev. Lett.* **100**, 137001 (2008).
- ⁴A. Lanzara, P. V. Bogdanov, X. J. Zhou, S. A. Kellar, D. L. Feng, E. D. Lu, T. Yoshida, H. Eisaki, A. Fujimori, K. Kishio, J.-I. Shimoyama, T. Noda, S. Uchida, Z. Hussain, and Z.-X. Shen, *Nature (London)* **412**, 510 (2001).
- ⁵X. J. Zhou, J. R. Shi, T. Yoshida, T. Cuk, W. L. Yang, V. Brouet, J. Nakamura, N. Mannella, S. Komiya, Y. Ando, F. Zhou, W. X. Ti, J. W. Xiong, Z. X. Zhao, T. Sasagawa, T. Kakeshita, H. Eisaki, S. Uchida, A. Fujimori, Z. Y. Zhang, E. W. Plummer, R. B. Laughlin, Z. Hussain, and Z.-X. Shen, *Phys. Rev. Lett.* **95**, 117001 (2005).
- ⁶T. P. Devereaux, T. Cuk, Z.-X. Shen, and N. Nagaosa, *Phys. Rev. Lett.* **93**, 117004 (2004).
- ⁷D. Reznik, L. Pintschovius, M. Ito, S. Iikubo, M. Sato, H. Goka, M. Fujita, K. Yamada, G. D. Gu, and J. M. Tranquada, *Nature (London)* **440**, 1170 (2006).
- ⁸R. J. McQueeney, Y. Petrov, T. Egami, M. Yethiraj, G. Shirane, and Y. Endoh, *Phys. Rev. Lett.* **82**, 628 (1999).
- ⁹L. Pintschovius and M. Braden, *Phys. Rev. B* **60**, R15039 (1999).
- ¹⁰H. Uchiyama, A. Q. R. Baron, S. Tsutsui, Y. Tanaka, W. Z. Hu, A. Yamamoto, S. Tajima, and Y. Endoh, *Phys. Rev. Lett.* **92**, 197005 (2004).
- ¹¹T. Fukuda, J. Mizuki, K. Ikeuchi, K. Yamada, A. Q. R. Baron, and S. Tsutsui, *Phys. Rev. B* **71**, 060501(R) (2005).
- ¹²J. Zaanen and O. Gunnarsson, *Phys. Rev. B* **40**, 7391 (1989).
- ¹³S. A. Kivelson, I. P. Bindloss, E. Fradkin, V. Oganesyan, J. M. Tranquada, A. Kapitulnik, and C. Howald, *Rev. Mod. Phys.* **75**, 1201 (2003).
- ¹⁴J. M. Tranquada, B. J. Sternlieb, J. D. Axe, Y. Nakamura, and S. Uchida, *Nature (London)* **375**, 561 (1995).
- ¹⁵D. Reznik, L. Pintschovius, M. Fujita, K. Yamada, G. D. Gu, and J. M. Tranquada, *J. Low Temp. Phys.* **147**, 353 (2007).
- ¹⁶J.-H. Chung, T. Egami, R. J. McQueeney, M. Yethiraj, M. Arai, T. Yokoo, Y. Petrov, H. A. Mook, Y. Endoh, S. Tajima, C. Frost, and F. Dogan, *Phys. Rev. B* **67**, 014517 (2003).
- ¹⁷L. Pintschovius, D. Reznik, W. Reichardt, Y. Endoh, H. Hiraka, J. M. Tranquada, H. Uchiyama, T. Masui, and S. Tajima, *Phys. Rev. B* **69**, 214506 (2004).
- ¹⁸D. Reznik, L. Pintschovius, W. Reichardt, Y. Endoh, H. Hiraka, J. M. Tranquada, S. Tajima, H. Uchiyama, and T. Masui, *J. Low Temp. Phys.* **131**, 417 (2003).
- ¹⁹D. Reznik, P. Bourges, L. Pintschovius, Y. Endoh, Y. Sidis, T. Masui, and S. Tajima, *Phys. Rev. Lett.* **93**, 207003 (2004).
- ²⁰W. Reichardt, *J. Low Temp. Phys.* **105**, 807 (1996).
- ²¹F. Stercel, T. Egami, H. A. Mook, M. Yethiraj, J.-H. Chung, M. Arai, C. Frost, and F. Dogan, *Phys. Rev. B* **77**, 014502 (2008).
- ²²L. Pintschovius, W. Reichardt, M. Kläser, T. Wolf, and H. v. Löhneysen, *Phys. Rev. Lett.* **89**, 037001 (2002).
- ²³B. Renker, H. Rietschel, L. Pintschovius, W. Gläser, P. Brüesch, D. Kuse, and M. J. Rice, *Phys. Rev. Lett.* **30**, 1144 (1973).
- ²⁴W. E. Pickett, R. E. Cohen, and H. Krakauer, *Phys. Rev. B* **42**, 8764 (1990).
- ²⁵D. J. Derro, E. W. Hudson, K. M. Lang, S. H. Pan, J. C. Davis, J. T. Markert, and A. L. de Lozanne, *Phys. Rev. Lett.* **88**, 097002 (2002).
- ²⁶M. Maki, T. Nishizaki, K. Shibata, and N. Kobayashi, *Phys. Rev. B* **65**, 140511(R) (2002).
- ²⁷V. B. Zabolotnyy, S. V. Borisenko, A. A. Kordyuk, J. Geck, D. S. Inosov, A. Koitzsch, J. Fink, M. Knupfer, B. Buchner, S.-L. Drechsler, H. Berger, A. Erb, M. Lambacher, L. Patthey, V. Hinkov, and B. Keimer, *Phys. Rev. B* **76**, 064519 (2007).
- ²⁸V. Zabolotnyy, Ph.D. thesis, IFW-Dresden (unpublished).
- ²⁹K. Nakayama, T. Sato, K. Terashima, H. Matsui, T. Takahashi, M. Kubota, K. Ono, T. Nishizaki, Y. Takahashi, and N. Kobayashi, *Phys. Rev. B* **75**, 014513 (2007).
- ³⁰K. Park and S. Sachdev, *Phys. Rev. B* **64**, 184510 (2001).
- ³¹E. Kaneshita, M. Ichioka, and K. Machida, *Phys. Rev. Lett.* **88**, 115501 (2002).
- ³²H. A. Mook, P. Dai, F. Doğan, and R. D. Hunt, *Nature (London)* **404**, 729 (2000).
- ³³C. Stock, W. J. L. Buyers, R. Liang, D. Peets, Z. Tun, D. Bonn, W. N. Hardy, and R. J. Birgeneau, *Phys. Rev. B* **69**, 014502 (2004).
- ³⁴V. Hinkov, P. Bourges, S. Pailhes, Y. Sidis, A. Ivanov, C. D. Frost, T. G. Perring, C. T. Lin, D. P. Chen, and B. Keimer, *Nat. Phys.* **3**, 780 (2007).
- ³⁵V. Hinkov, D. Haug, B. Fauqué, P. Bourges, Y. Sidis, A. Ivanov, C. Bernhard, C. T. Lin, and B. Keimer, *Science* **319**, 597 (2008).
- ³⁶S. A. Kivelson, E. Fradkin, and V. J. Emery, *Nature (London)* **393**, 550 (1998).
- ³⁷M. Granath, V. Oganesyan, D. Orgad, and S. A. Kivelson, *Phys. Rev. B* **65**, 184501 (2002).
- ³⁸T. Valla, A. V. Federov, J. Lee, J. C. Davis, and G. D. Gu, *Science* **314**, 1914 (2006).
- ³⁹H. A. Mook, M. Yethiraj, G. Aeppli, T. E. Mason, and T. Arm-

- strong, Phys. Rev. Lett. **70**, 3490 (1993).
- ⁴⁰H. F. Fong, B. Keimer, D. Reznik, D. L. Milius, and I. A. Aksay, Phys. Rev. B **54**, 6708 (1996).
- ⁴¹P. Bourges, L. P. Regnault, Y. Sidis, and C. Vettier, Phys. Rev. B **53**, 876 (1996).
- ⁴²S. Wakimoto, H. Kimura, K. Ishii, K. Ikeuchi, T. Adachi, M. Fujita, K. Kakurai, Y. Koike, J. Mizuki, Y. Noda, A. H. Said, Y. Shvyd'ko, and K. Yamada, arXiv:0806.3302 (unpublished).